E3S Web of Conferences **551**, 03002 (2024) https://doi.org/10.1051/e3sconf/202455103002
EEPES 2024

Design and simulation of bidirectional DC-DC converter topology for battery applications

Mehmet Kurtoğlu[1*], and *Fatih* Eroğlu[2]

[1]Iskenderun Technical University, Dept. of Electrical and Electronics Eng., Hatay, 31200, Turkey
[2]TOFAŞ Türk Otomobil Fabrikası A.Ş., R&D, Propulsion Systems Management, Bursa, 16100, Turkey

Abstract. Recently, energy storage has become a significant topic for renewable energy based power system applications. Batteries are one of the most popular energy storage devices adopted by renewable energy sources, electrical vehicles and grid connected systems. In this context, the bidirectional DC-DC converter (BDC) enables bidirectional power flow by controlling the charging and discharging stage of the battery in battery applications. Accordingly, the battery current is regulated through the duty cycle of the BDC considering the state of charge of the battery and current direction. In this study, a non-isolated BDC, has a buck and boost principle of operation, is designed, analysed and simulated under various case studies. In the designed system, BDC controls the bidirectional power flow between the battery and DC link. Specifically, in the charging stage of battery operating in buck mode, DC-link supplies the power to the battery and BDC regulates the battery current using proportional-integral (PI) controller. On the other hand, in the discharging stage of the battery operating in boost mode, when DC source is disconnected, the battery supplies the power to DC load and DC-link voltage is controlled by the BDC via PI controller. The simulation results are presented to show the operation and control of the BDC under different scenarios.

1 Introduction

The significance of energy storage systems has increased due to the growing capacity of renewable energy sources in power generation and the development of electric vehicles in the transportation sector [1-3]. Energy storage devices such as batteries or supercapacitors are extensively used to store energy from the renewable sources and supply power to the load demand [4, 5].

Batteries are considered to be the best energy storage technology because of their availability and quick response [6]. Accordingly, the charging and discharging process of battery is important in terms of reliable operation. The bidirectional DC-DC converter (BDC) is used as an interface circuit between power generation unit and battery to control the charging and discharging mode of operation of battery [7]. BDC topology has distinguishing features such as bidirectional power flow, transformer-less operation and

* Corresponding author: mehmet.kurtoglu@iste.edu.tr

efficient performance [8]. Owing to its exceptional features, BDC is adopted in battery energy storage system (BESS) applications.

In the existing literature, research presented in [9] reports the design and analysis of BDC based solar photovoltaic (PV) system. The bidirectional buck-boost operation is shown with open loop control using simulation results.

In [10], a detailed loss analysis and theoretical model to determine the efficiency of the BDC are studied. Also, converter's efficiency is analysed in terms of the effect of temperature, switching frequency and duty ratio. Experimental findings are given to demonstrate the feasibility of the developed model.

A logic control scheme is developed for BDC based BESS in [11]. The small signal model for buck and boost operation is presented to control the BDC via averaging and linearization technique. Simulation tests are performed to show the performance of the designed control scheme.

Reference [12] suggests a time delay control as a solution to address the nonlinear characteristics of BDC based lithium-ion battery application. To show the superior performance of the designed controller, it is compared with proportional-integral (PI) control and the experimental implementation is carried out for verification.

Research reported in [13] presents the design and modeling of a solar PV electrical vehicle based on BDC. A control method is introduced by giving simulation results under various atmospheric conditions.

In this paper, a non-isolated BDC with a buck and boost operating concept is designed and simulated through a number of case studies. Within the designed system, the BDC controls the bidirectional power flow between battery and DC-link. During the charging stage of a battery working in buck mode, the battery is fed from the DC-link, and the battery current is regulated by the BDC through the use of PI controller. Conversely, in the discharge stage of the battery operating in boost mode, when the DC source is disconnected, the battery supplies power to the DC load. The BDC ensures the control of the DC-link voltage using PI controller during this process. The operation and control of the BDC is shown by the simulation results under various scenarios.

Including this introductory section, the overall structure of the study consists of four sections. Section 2 explains the circuit structure, operation and control of BDC with battery application. Simulation study of BDC is reported in Section 3. Lastly, the conclusions are presented in Section 4.

2 BDC topology and battery application

The circuit configuration of the non-isolated BDC topology is represented in Figure 1. There are several advantages of this topology such as allowing the bidirectional energy transfer, compact size and high efficiency [14, 15]. As given in Figure 1, BDC has two switching elements (S_1 and S_2), two diodes (D_1 and D_2), two capacitors (C_1 and C_2) and one inductor (L). MOSFET or IGBT can be used as a switching element in the circuit implementation of this topology. Basically, in order to transfer the energy in two directions, BDC can operate in buck and boost mode.

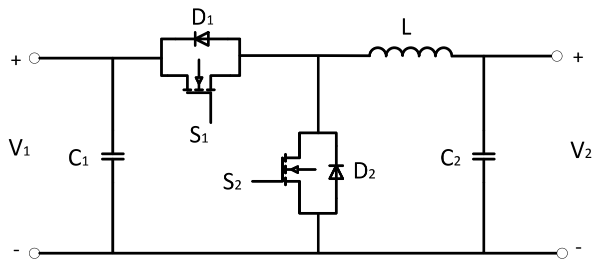

Fig. 1. Circuit structure of the BDC topology.

2.1 Buck mode operation

In this mode, BDC operates in the forward operation mode. The energy is transferred from the source V_1 to the V_2 side. The relation between input voltage (V_1) and output voltage (V_2) is given as

$$k_{D1} = \frac{V_2}{V_1} \quad (1)$$

where k_{D1} denotes the duty cycle. Direction of the inductor current (i_L) is from left to right. In the buck mode, there are two operating cases depending on the switching time (T_s). When $0 \leq t \leq k_{D1}T_s$, S_1 is ON, S_2 is OFF and i_L is increasing. Conversely, when $k_{D1}T_s \leq t \leq T_s$, S_1 is OFF, S_2 is ON and i_L is decreasing. The current path for two cases is illustrated in Figure 2(a) and 2(b).

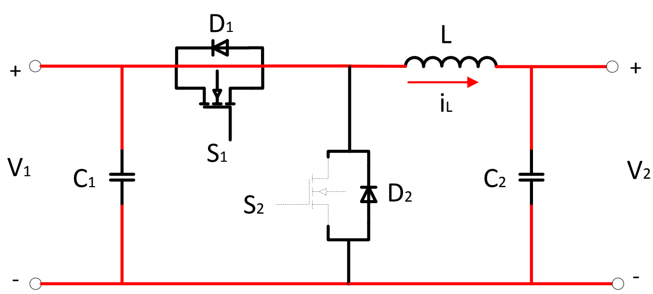

(a) $0 \leq t \leq k_{D1}T_s$

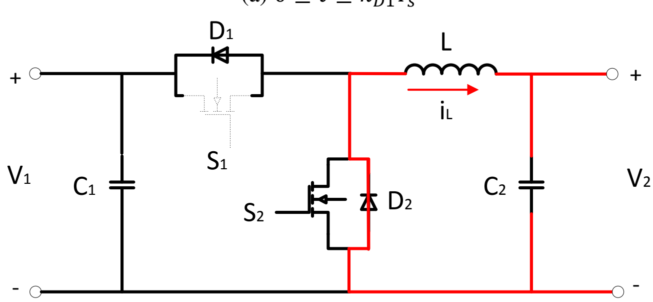

(b) $k_{D1}T_s \leq t \leq T_s$

Fig. 2. Buck mode operation cases.

2.2 Boost mode operation

In this mode, BDC operates in the backward operation mode. The energy stored in the inductor and V_2 power source such as battery supplies to the DC load in the V_1 part. The relation between input voltage (V_2) and output voltage (V_1) is expressed as

$$\frac{1}{1-k_{D2}} = \frac{V_1}{V_2} \tag{2}$$

where k_{D2} represents the duty cycle. Direction of the i_L is from right to left. In the boost mode, there are two operating cases depending on the T_s. When $0 \le t \le k_{D2}T_s$, S_1 is OFF, S_2 is ON and i_L is increasing. Conversely, when $k_{D2}T_s \le t \le T_s$, S_1 is ON, S_2 is OFF and i_L is decreasing. The current path for two cases is shown in Figure 3(a) and 3(b).

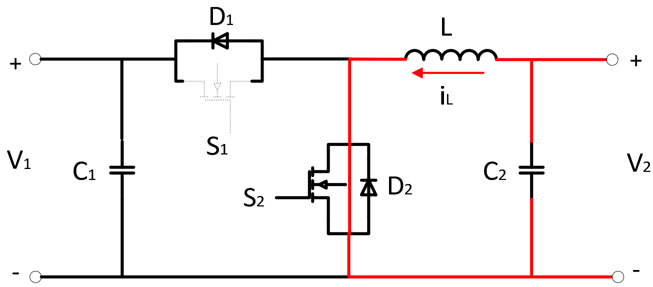

(a) $0 \le t \le k_{D2}T_s$

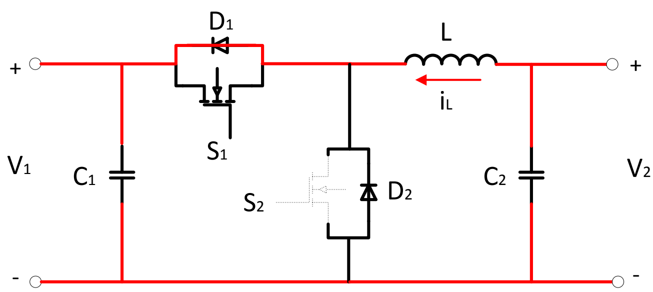

(b) $k_{D2}T_s \le t \le T_s$

Fig. 3. Boost mode operation cases.

The schematic diagram of power system including BDC and battery is demonstrated in Figure 4. While any renewable energy source such as wind and solar power can be used as voltage source, simple DC power source is also employed. DC load is fed from the DC-link whose energy is supplied from voltage source or battery. In this configuration, BDC controls the battery current in a bidirectional manner. In buck mode operation, while battery is charging, load is fed from the voltage source. On the other hand, in boost mode operation, during the disconnection of voltage source, while battery is discharging, load is fed from the battery.

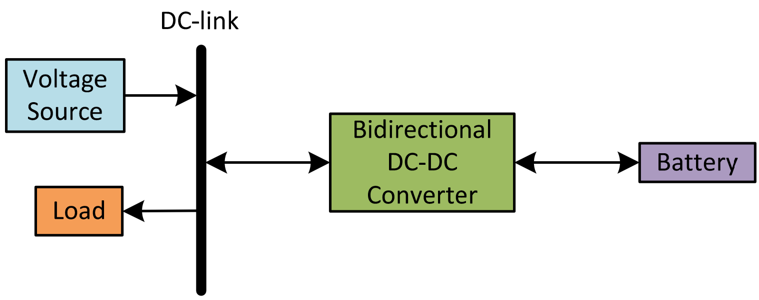

Fig. 4. Overall schematic diagram of BDC with battery system.

Figure 5 shows the control block diagram of buck mode operation. Voltage source is enabled on DC-link side and battery is charging by regulating the battery current using PI controller. In addition, control scheme for boost mode operation is presented in Figure 6. Accordingly, when the voltage source is disabled or unavailable due to the external conditions, DC-link and load is fully fed from the battery.

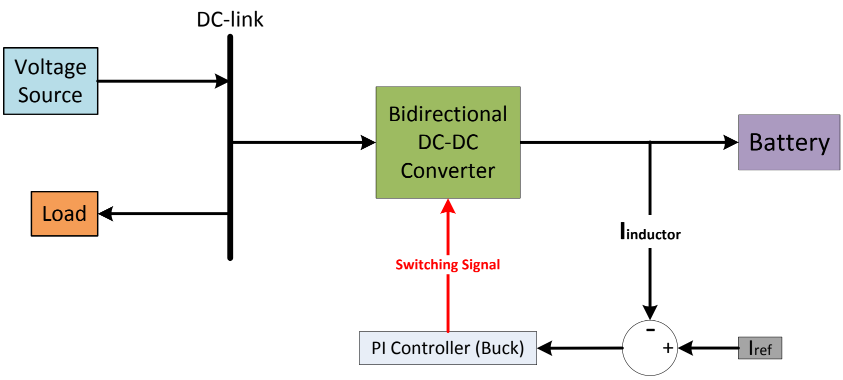

Fig. 5. Control loop for buck (charging) mode.

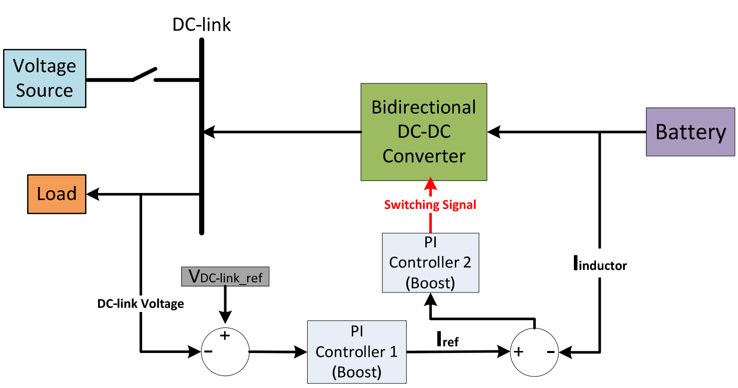

Fig. 6. Control loop for boost (discharging) mode.

Table 1. Design parameters.

Parameter	**Value**	**Parameter**	**Value**
Voltage source (V_1)	120 V	Battery type	Lithium-ion
Battery voltage	48 V	Battery capacity	100 Ah
Switching frequency	15 kHz	Battery initial SOC	50
DC-link capacitance	10 mF	Load resistance	10 •
Inductor (L)	10 mH	Load inductance	5 mH

Table 2. Controller parameters.

Control Unit	**Value**
PI controller (Buck)	Kp=0.004 Ki=9.5
PI controller 1 (Boost)	Kp=0.02 Ki=6
PI controller 2 (Boost)	Kp=0.002 Ki=0.6

3 Simulation study

BDC based BESS is designed and simulated under various scenarios in this work. Circuit parameters of the designed model are given in Table 1. Controller parameters of the designed system are given in Table 2. All simulations are conducted under RL load condition, which is connected to DC-link side of the BDC.

3.1 Buck mode operation

3.1.1 Case Study 1: Constant reference current

In this case, the power is transferred from DC-link to the battery. Accordingly, the simulation is conducted with constant reference current mode. Control loop given in Figure 5 is activated by setting the reference current to 20 A. Figure 7(a) and 7(b) show the battery voltage (approximately 51.9 V) and battery current (-20 A), respectively. From those values, the power absorbed by the battery is nearly equal to 1038 W. According to the Figure 8, the BDC inductor current follows the reference set current as 20 A. Battery state-of-charge (SOC) is increasing at a constant rate meaning that the battery is charging, as given in Figure 9.

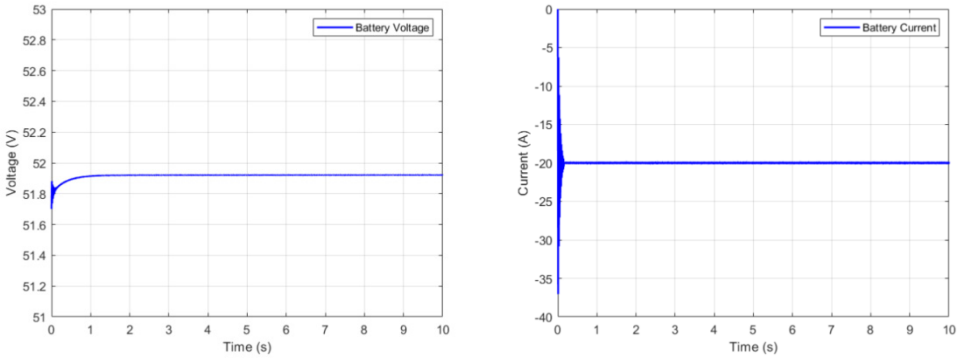

(a) (b)

Fig. 7. (a) Battery voltage, (b) battery current on case 1 for buck mode.

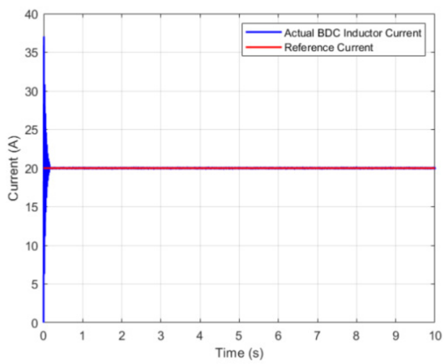

Fig. 8. BDC inductor current and reference current on case 1 for buck mode.

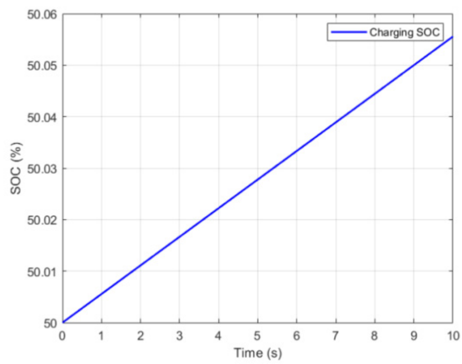

Fig. 9. Battery SOC on case 1 for buck mode.

3.1.2 Case Study 2: Variable reference current

In this scenario, the power is also transferred from DC-link to the battery. The simulation is done with variable reference current mode. Control scheme presented in Figure 5 is activated by setting the reference current to 20 A, 40 A, 10 A and 30 A, respectively. The controller reference current change is determined by selecting 4 s time intervals. Figure 10(a) and 10(b) demonstrate the battery voltage and battery current, respectively. While battery voltage is around 52 V, battery current is regulated at -20 A, -40 A, -10 A and -30 A, respectively. From those values, the power absorbed by the battery is nearly equal to 1038 W, 2086 W, 518 W and 1563 W, respectively. According to the Figure 11, the BDC inductor current follows the reference set current during the whole simulation. Battery SOC is increasing at different rates meaning that the battery is charging, as given in Figure 12.

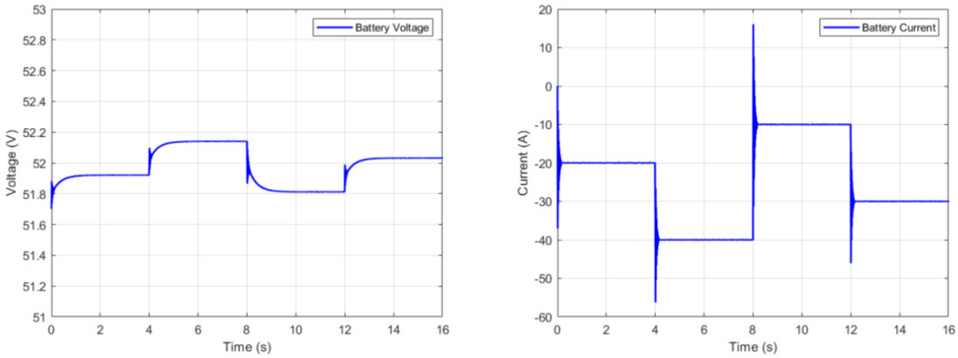

(a) (b)

Fig. 10. Battery voltage (a), battery current (b) on case 2 for buck mode.

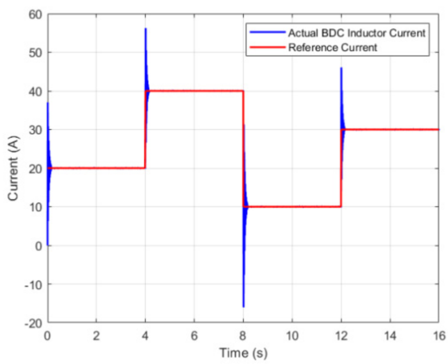

Fig. 11. BDC inductor current and reference current on case 2 for buck mode.

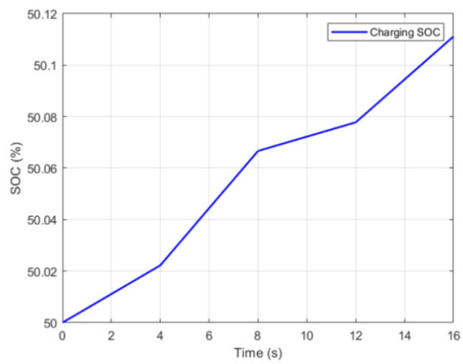

Fig. 12. Battery SOC on case 2 for buck mode.

3.2 Boost mode operation

3.2.1 Case Study 1: Constant DC-link voltage

The power is transferred from battery to the load in this case analysis. The simulation is carried out with constant DC-link voltage mode. Control scheme depicted in Figure 6 is activated by setting the reference DC-link voltage to 120 V. Figure 13(a) and 13(b) show the battery voltage (approximately 51,36 V) and battery current (29 A), respectively. From those values, the power delivered by the battery is nearly equal to 1489 W. According to the Figure 14, DC-link voltage follows the reference voltage as 120 V. Battery SOC is decreasing at a constant rate meaning that the battery is discharging, as given in Figure 15.

https://doi.org/10.1051/e3sconf/202455103002

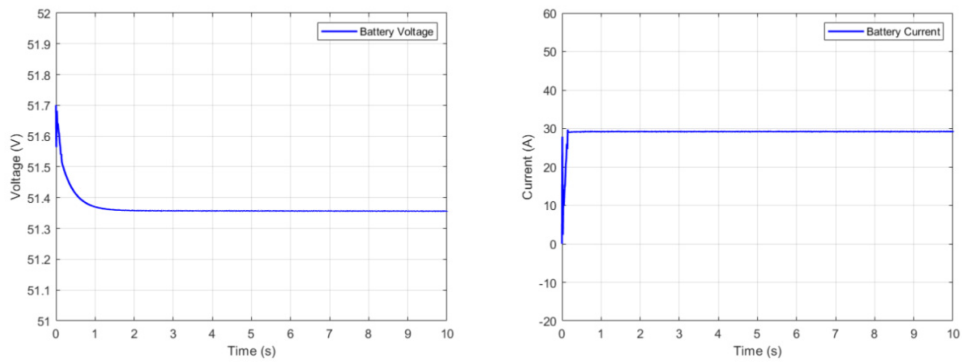

(a) (b)

Fig. 13. Battery voltage (a), battery current (b) on case 1 for boost mode.

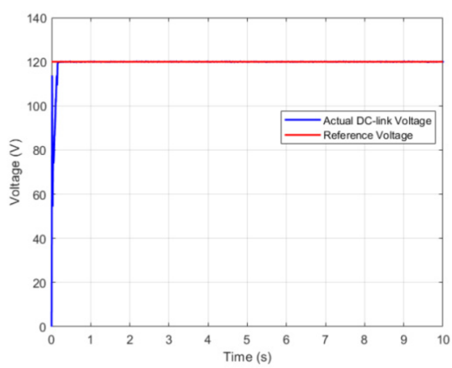

Fig. 14. DC-link voltage and reference voltage on case 1 for boost mode.

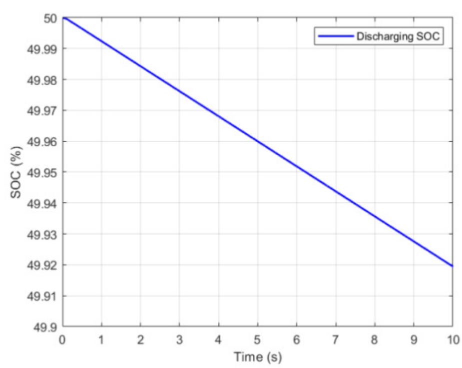

Fig. 15. Battery SOC on case 1 for boost mode.

3.2.2 Case Study 2: Variable DC-link voltage

The power is also transferred from battery to the load in this case analysis. The simulation is conducted with variable DC-link voltage mode. Control scheme presented in Figure 6 is activated by setting the reference DC-link voltage to 120 V, 140 V, 100 V and 130 V, respectively. The controller reference voltage change is specified by selecting 4 s time intervals. Figure 16(a) and 16(b) show the battery voltage and battery current, respectively. While battery voltage is around 51.3 V, battery current is nearly regulated at 30 A, 40 A, 20 A and 35 A, respectively. From those values, the power delivered by the battery is nearly equal to 1539 W, 2052 W, 1026 W and 1795 W, respectively.

https://doi.org/10.1051/e3sconf/202455103002

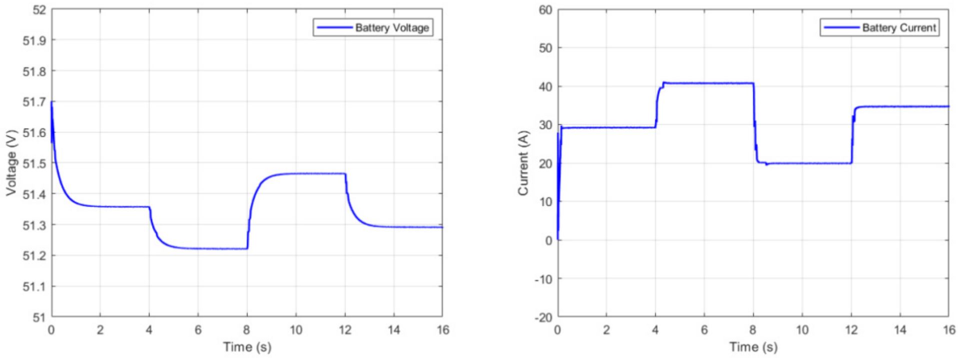

(a) (b)

Fig. 16. Battery voltage (a), battery current (b) on case 2 for boost mode.

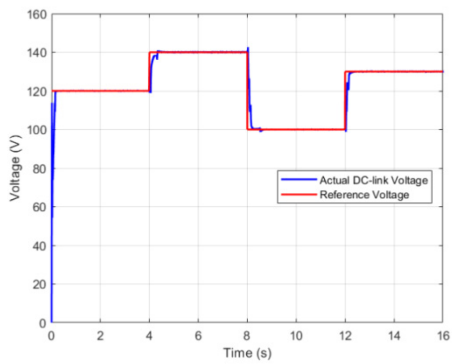

Fig. 17. DC-link voltage and reference voltage on case 2 for boost mode.

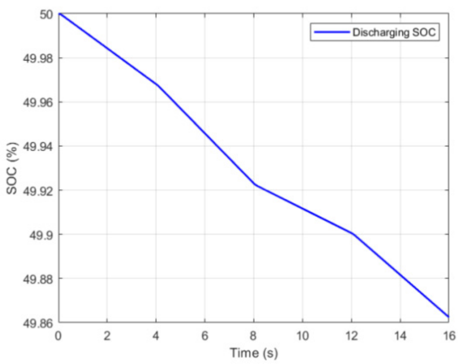

Fig. 18. Battery SOC on case 2 for boost mode.

According to the Figure 17, DC-link voltage follows the reference voltage during the whole simulation. Battery SOC is decreasing at different rates meaning that the battery is discharging, as given in Figure 18.

4 Conclusion

Over the past few decades, energy storage has gained importance for power electronics applications based on renewable energy sources. Batteries are an attractive choice for energy storage and they are widely adopted by renewable energy sources, electrical vehicles and grid connected systems. In battery applications, bidirectional power flow control by regulating the charging and discharging stage of battery is achieved by BDC. Accordingly, the battery current is controlled by adjusting the duty cycle of the BDC by taking into account the state of charge of the battery and current direction. In this work, a non-isolated BDC, has a buck and boost principle of operation, has been designed, analyzed and simulated under various scenarios. In the simulated system, BDC controls the bidirectional power flow between battery and DC link. In this context, in buck mode, battery has been fed from the DC-link and the battery current has been controlled via PI controller. On the other hand, in boost mode, when DC source is disconnected, DC load has been fed from the battery and DC-link voltage is regulated by BDC using PI controller. The simulation results have been presented to demonstrate the operation and control of the BDC under different case studies.

References

1. A. A. Kebede, T. Kalogiannis, J. Van Mierlo, M. Berecibar, A comprehensive review of stationary energy storage devices for large scale renewable energy sources grid integration, Renew. Sustain. Energy Rev., **159**, p. 112213, (2022)
2. Y. Sun, Z. Zhao, M. Yang, D. Jia, W. Pei, B. Xu, Overview of energy storage in renewable energy power fluctuation mitigation, CSEE J. Power Energy Syst., **6** (1), pp. 160–173, (2020)
3. S. Hajiaghasi, A. Salemnia, M. Hamzeh, Hybrid energy storage system for microgrids applications: A review, J. Energy Storage, **21**, pp. 543–570, (2019)
4. A. G. Olabi, C. Onumaegbu, T. Wilberforce, M. Ramadan, M. A. Abdelkareem, A. H. Al – Alami, Critical review of energy storage systems, Energy, **214**, p. 118987, (2021)
5. M. M. Rahman, A. O. Oni, E. Gemechu, A. Kumar, Assessment of energy storage technologies: A review, Energy Convers. Manag., **223**, no. May, p. 113295, (2020)
6. N. Padmanabhan, M. Ahmed, and K. Bhattacharya, Battery Energy Storage Systems in Energy and Reserve Markets, IEEE Trans. Power Syst., **35** (1), pp. 215–226, (2020)
7. R. Rajasekaran & P. U. Rani, Bidirectional DC-DC Converter for Microgrid in Energy Management System, Int. J. Electron., **108** (2), pp. 1–22, (2020)
8. T. Sutikno, R. A. Aprilianto, and H. S. Purnama, Application of non-isolated bidirectional DC–DC converters for renewable and sustainable energy systems: a review, Clean Energy, **7** (2), pp. 293–311, (2023)
9. S. Jadhav, N. Devdas, S. Nisar, V. Bajpai, *Bidirectional DC-DC converter in Solar PV System for Battery Charging Application*, in Proceeding of 2018 Int. Conf. Smart City Emerg. Technol. ICSCET 2018, (2018)
10. C. Wang, R. Xiong, H. He, X. Ding, W. Shen, Efficiency analysis of a bidirectional DC/DC converter in a hybrid energy storage system for plug-in hybrid electric vehicles, Appl. Energy, **183**, pp. 612–622, (2016)
11. R. Pramanik, B. B. Pati, Modelling and control of a non-isolated half-bridge bidirectional DC-DC converter with an energy management topology applicable with EV/HEV, J. King Saud Univ. - Eng. Sci., **35** (2), pp. 116–122, (2021)
12. Y. X. Wang, F. F. Qin, Y. B. Kim, Bidirectional DC-DC converter design and implementation for lithium-ion battery application, Asia-Pacific Power Energy Eng. Conf. APPEEC, **2015**, pp. 0–4, (2014)
13. S. Aragon-Aviles, A. H. Kadam, T. Sidhu, S. S. Williamson, Modeling, Analysis, Design, and Simulation of a Bidirectional DC-DC Converter with Integrated Snow Removal Functionality for Solar PV Electric Vehicle Charger Applications, Energies, **15** (8), (2022)
14. P. Vishnuram et al., A comprehensive review on EV power converter topologies charger types infrastructure and communication techniques, Front. Energy Res., **11**, pp. 1–17, (2023)
15. V. Viswanatha & R. Venkata, Microcontroller based bidirectional buck–boost converter for photo-voltaic power plant, J. Electr. Syst. Inf. Technol., **5** (3), pp. 745–758, (2018)